Cell Biochem Biophys (2007) 47:361–375
DOI 10.1007/s12013-007-0031-8

ORIGINAL PAPER

Understanding antibody–antigen associations by molecular dynamics simulations: Detection of important intra- and inter-molecular salt bridges

Neeti Sinha · Yili Li · Claudia A. Lipschultz · Sandra J. Smith-Gill

Published online: 18 April 2007

Abstract 1 NSec molecular dynamics (MD) simulation of anti-hen egg white antibody, HyHEL63 (HH63), complexed with HEL reveals important molecular interactions, not revealed in its X-ray crystal structure. These molecular interactions were predicted to be critical for the complex formation, based on structure–function studies of this complex and 3-other anti-HEL antibodies, HH8, HH10 and HH26, HEL complexes. All four antibodies belong to the same structural family, referred to here as HH10 family. Ala scanning results show that they recognize 'coincident epitopes'. 1 NSec explicit, with periodic boundary condition, MD simulation of HH63-HEL reveals the presence of functionally important salt-bridges. Around 200 ps in vacuo and an additional 20 ps explicit simulation agree with the observations from 1 Nsec simulation. Intra-molecular salt-bridges predicted to play significant roles in the complex formation, were revealed during MD simulation. A very stabilizing salt-bridge network, and another intra-molecular salt-bridge, at the binding site of HEL, revealed during the MD simulation, is proposed to predipose binding site geometry for specific binding. All the revealed salt-bridges are present in one or more of the other three complexes and/or involve ''hot-spot'' epitope and paratope residues. Most of these charged epitope residues make large contribution to the binding free energy. The ''hot spot'' epitope residue $Lys97_Y$, which significantly contributes to the free energy of binding in all the complexes, forms an intermolecular salt-bridge in several MD conformers. Our earlier computations have shown that this inter-molecular salt-bridge plays a significant role in determining specificity and flexibility of binding in the HH8-HEL and HH26-HEL complexes. Using a robust criterion of salt-bridge detection, this inter-molecular salt-bridge was detected in the native structures of the HH8-HEL and HH26-HEL complexes, but was not revealed in the crystal structure of HH63-HEL complex. The electrostatic strength of this revealed salt-bridge was very strong. During 1 Nsec MD simulation this salt-bridge networks with another inter-molecular salt-bridge to form an inter-molecular salt-bridge triad. Participation of $Lys97_Y$ in the formation of inter-molecular triad further validates the functional importance of $Lys97_Y$ in HH63-HEL associations. These results demonstrate that many important structural details of biomolecular interactions can be better understood when studied in a dynamic environment, and that MD simulations can complement and expand information obtained from static X-ray structure. This study also highlights ''hot-spot'' molecular interactions in HyHEL63-HEL complex.

Keywords Antibody–antigen associations · Molecular dynamics simulation · Salt-bridges · Hydrogen-bonds · Flexibility · Antibody binding site

N. Sinha (✉) · Y. Li · C. A. Lipschultz · S. J. Smith-Gill
Structural Biophysics Laboratory, Division of Basic Sciences, Bldg. 469 Frederick Cancer Research and Development Center, National Cancer Institute, National Institutes of Health, Frederick, MD 21702, USA
e-mail: nsinha@jhu.edu

Present Address:
N. Sinha
106-Mudd Hall, Johns Hopkins University, 3400 N. Charles Street, Baltimore, MD 21218, USA

Abbreviations

CDR	Complementarity-determining region
HH	HyHEL
HEL	Hen egg white lysozyme
PDB	Protein data bank

Introduction

Antibody–antigen complexes have been notable models to study underlying basics of protein-protein interactions and molecular recognition, both experimentally [1–7] and computationally [8–10]. Other protein complexes have also been studied to scrutinize the general principles of protein-protein interactions [11, 12]. These studies generally rely on structures determined by X-ray crystallography. Structure–function studies provide clues of how the subtle variations in antibody sequence predispose their structure to effectively distinguish widely diverse antigens, and how affinity maturation is acquired. Subtle variations in complementary determining regions of antibodies may lead to significant changes in their interaction thermodynamics with antigens. Proportions and distributions of charged/hydrophobic residues at binding sites lead to differentiations in binding mechanisms, playing major roles in molecular recognitions. Such studies also elucidate the general mechanism of protein–protein associations, such as in formation of protein complexes or in the operation of biomolecular cascades.

Macromolecular complexes, however, are known to be dynamic structures. Biological molecules in solution exhibit a range of conformations, in equilibrium with each other with low kinetic barriers between them. An X-ray crystal structure is a ''snapshot'', capturing one among several fluctuating conformations, and it is probable that all crucial molecular interactions are not revealed when looking at the just one conformation. Thus the static picture obtained by X-ray crystallography may not provide complete depictions of the molecule in solution. It is intuitive that important inter-molecular associations, like salt-bridge and hydrogen-bonds, fluctuate at association equilibria, and provide optimum balance of specificity and affinity with which protein–protein binds. In addition, protein structure is comprised of flexible and rigid regions. Flexible regions, or regions required to undergo movements for function, either lack or contain destabilizing or marginally stabilizing salt-bridges [13, 14]. NMR can reveal molecular dynamics (MD) of an interaction, but NMR is not possible at atomic resolution of such large protein-protein complexes. An alternate approach is to use MD simulations to obtain a dynamic profile of a complex. Comparison of a range of conformational isomers may identify such inherent flexible and rigid regions and the binding mechanisms. Inter-molecular and intra-molecular contacts formed and broken during MD simulation are thus expected to provide an insight into the dynamic behavior of the complex, and overcome any crystallization artifacts [15]. Here to complement the the X-ray structure of HH63-HEL complex [16] we utilize the MD approach to investigate antibody–antigen associations.

HH8, HH10, HH26, and HH63 are structurally and functionally related monoclonal antibodies specific for hen egg-white lysozyme (HEL) [16–19]. These antibodies share about 90% sequence identity with no insertions and deletions, and complementarity determining regions (CDRs) are of identical lengths [16, 20, 21]. Most sequence variations are due to somatic point mutations in the CDRs or joining mechanisms in CDR-H3 [22].They have high affinity towards HEL and recognize ''coincident'' epitopes on HEL (Fig. 1a): They compete with each other in antibody blocking assays, co-bind in complementation assays, and their binding affinity is reduced by mutations of same epitope residues [17, 19–23]. The HEL binding of HH63 has been described as more specific than HH10 and less specific than HH26 (16, 23, present work), and it is more sensitive towards epitope mutations than HH8 and HH10 (present work). We have proposed that the networking pattern and electrostatic strengths of salt-bridges determine cross reactivity and specificity in the binding of the HEL by the antibodies HH8, HH10, and HH26 [24].Salt-bridges have been shown to play important structural and functional roles in intermolecular interactions [25–28]. Their electrostatic strengths have been linked to protein stability and flexibility [14, 24, 29, 30]. We are, therefore, interested in investigating the numbers, the electrostatic strengths, and the networking pattern, if any, of salt-bridges in the HH63-HEL complex. However, applying rigourous atomic structural criteria for defining salt bridges [24], we found that some of the salt-bridges are not present in the HH63-HEL X-ray structure which would be expected from structural studies on the other complexes and from experimental observations. We, therefore, subjected the HH63-HEL complex to MD simulation to probe time-resolved details of inter and intra-molecular salt-bridges, and their electrostatic properties.

We describe here the details of salt-bridge interactions in HH63-HEL complex during the time course of the MD simulation, in the range of conformational isomers around the native state binding site. The work demonstrates that complete details of molecular interactions can only be seen in dynamics. During MD simulation important inter- and intra-molecular salt-bridges were revealed. We compare the salt-bridge interactions in the conformers extracted from MD trajectory with the salt-bridges present in the other three antibody–antigen complexes, and show that many dynamic interactions revealed during the HH63-HEL MD simulations are also found in complexes of one or

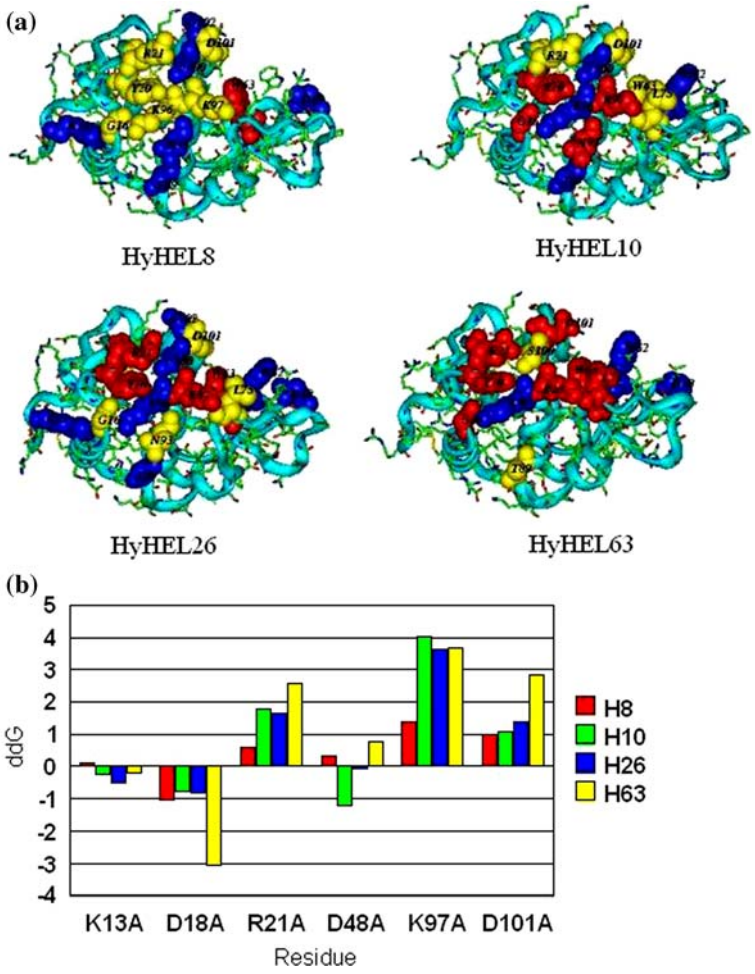

Fig. 1 Alanine scanning of epitope residues in HH8-HEL [48], HH10-HEL (pdb id-3hfm), HH26-HEL [Model-Mohan et al. [48] and HH63-HEL (pdb id-1dqj) complexes. (**a**) This illustrate the qualitative differences in the binding energy contributions of epitope residues in the four HH-HEL complexes, defined as $\Delta\Delta G_{mut-wild}$. The epitope residues contributing –0.2 kcal/mol or more are shown in CPK representations. Epitope residues contributing ≥–2.0 kcal/mol, –1 to –2.0 kcal/mol and –0.2 to –1.0 kcal/mol are shown in red, yellow and blue colors, respectively. The side-chains of the remaining residues are displayed in stick model, and are colored by atom type. (**b**) It shows free energy contributions of the charged epitope residues

more of the other three antibodies. Epitope residues participating in these salt bridges were also identified as ''hot spot'' residues in alanine scanning binding experiments, demonstrating their functional importance. MD simulation of HH63-HEL complex revealed ''hot-spot'' molecular inetractions. Our continuum electrostatic calculations on the revealed salt-bridges further highlight a possible binding mechanism operating in HH63-HEL, and in the other three complexes. These results complement and extend the observation made from X-ray crystal structures of HH63 complexed with HEL and its mutants [16, 31, 32].

Materials and methods

Co-ordinates of HH63-HEL complex

The co-ordinates of HH63-HEL complex were extracted from the protein data bank [33], PDB ID- 1dqj. The complex of light chain (107 residues) and heavy chain (110 residues) variable domains with HEL is analyzed here. The complex was subjected to energy minimizations before the structural analysis and MD calculations were then performed. The energy minimization was performed using Conjugate Gradient (Polak-Ribiere) method, employing CVFF Force Field, with the final convergence value of 0.001, using the CDiscover module of Insight II (Molecular Simulations Inc.). The total potential energy after 1,000 interactions was –1,951.674 kcal/mol from the initial 39,019.318 kcal/mol of the X-ray structure. The minimized structure was used for the analysis presented here. The energy minimizations were performed to correct any short and/or unfavorable contacts. The inter-molecular interactions between HH63-HEL and energy minimized HH63-HEL were not significantly different (data not shown).

Molecular dynamics simulation

1Nsec MD simulation trajectory was taken from previously published work [34]. Molecular dynamics simulations were performed at constant temperature and volume, in NVT canonical ensemble, using velocity scaling method for temperature control, in the cubic periodic boundary conditions, using C-DISCOVER at the INSIGHT-II interface.

The initial velocities for all atoms were taken from Maxwellian distribution at the temperature of 298.0 K, employing the Verlet algorithms with a time step of 1 fs. The distance dependent dielectric was employed, with the protein dielectric value of 4.0. Group based cutoffs at 9.50 Å was used for the treatment of non-bonded interactions. System consisted of variable domains, lysozyme, water molecules in the crystal structure, and another 7,286 water molecules, making a total of 27,105 atoms per unit cell. All the atoms in the system were considered explicitly, and the interactions were computed using CFF91 force field. The system was subjected for equilibration for 10 Ps, before collecting data. About 1 ns MD was performed in five steps of 200 ps simulation each. The initial velocities for all atoms were taken from Maxwellian distribution at the temperature of 298.0 K, employing the Verlet algorithms with a time step of 1 fs. The dynamics, after each 200 ps step, was continued using the restart file, which contains all the internal co-ordinates and potential functions of the last conformation. The current velocity was used with the restart file while continuing the MD. Total energy, potential energy, kinetic energy and temperature showed steady behavior over the production run, suggesting that the sound equilibration was attained during the data collection stages [34]. C-α RMSD between first and final conformation was 1.72 Å. and 20 conformations at regular time interval (every 5 ps) were extracted from the last 200 ps stage of 1Nsec simulation, and analyzed for salt-bridge interactions.

Additional MD calculations were performed using the C-DISCOVER module of INSIGHT II, mainly to verify the observations from 1 Nsec simulation. The simulations were carried out in NVT (canonical) ensemble, using velocity scaling method for temperature control. Cell Multipole method (CMM) [35, 36], available in CDiscover, was used for the treatment of non-bonded interactions. The distance dependent dielectric was employed, with the protein dielectric value of 4.0. The initial velocities for all atoms were taken from Maxwellian distribution at the temperature of 298.0 K, employing the Verlet algorithms with a time step of 1 fs. The system was subjected for equilibration for 100 ps, before the data collection. The current velocity were then used, after 100 ps equilibration, for another 100 ps MD simulation (the production run), and the output were executed at every 10 step. The co-ordinates (snap-shots from the MD trajectory) were, however, saved at every 1,000 fs. All atoms were considered explicitly, and their interactions were computed using the CFF91 force field [37]. The system contained all six CDRs, with three bordering residues on both the sides of all CDRs, and all epitope residues and their bordering residues of HEL. The system included the complete interface residues of HH63 and HEL along with bordering residues within about 30.00 Å distance on all sides. Total energy, potential energy, kinetic energy and temperature showed steady behavior over the production run, suggesting that the sound equilibration was attained during the initial 100 ps equilibration run (data not shown; 34).

An additional 20 ps explicit simulation was performed with all of the above conditions except that the system contained all the atoms of light chain variable domain, heavy chain variable domain, HEL soaked in water. The explicit simulation also contained those water molecules which were part of the X-ray crystal structure [16]. The complex was soaked in a sphere of 25 water, which contained 2,114 water molecules, taking CDR-L3 residue position 93 as a center for the sphere, using SOAK of the VIEWER module of INSIGHT II. Soaking is accomplished by placing the molecule in an equilibrated three-dimensional grid of solvent and removing those solvent molecules which overlap with atoms in the molecule being solvated. MD simulation of this system was performed by subjecting all the atoms (antibody–antigen complex + water) to the initial velocity from Maxwellian distribution at the temperature of 298.0 K, employing the Verlet algorithms with a time step of 1 fs. The equilibration was performed for 10 ps. Velocity from 10 ps stage was then used for the 10 ps production run and data was collected. Large numbers of water molecules were retained around the complex in the last conformer of the MD trajectory, at 20 ps time step. The output was executed at every 10 fs time step. The snap-shots of trajectories were saved at every 1,000 fs. The water molecules were removed from the saved conformers before analyzing, to save the extra disk space.

Hydrogen-bonds and salt-bridges

The presence of a hydrogen bond is inferred when two non-hydrogen atoms with opposite partial charges are within a distance of 3.6 Å. Salt-bridges are inferred upon meeting the two criteria: 1) The centroid of the side-chain oppositely charged groups, like carboxylic group in glutamic acid and amino group in lysine, are within 4.0 Å; 2) aspartate or glutamate side-chain oxygen atoms are within 4.0 Å distance from nitrogen atoms of arginine, lysine or histidine side-chains. When for the same pair of residues there are more than one pair of nitrogen–oxygen atoms present within, the salt-bridge has been counted only once.

Electrostatic strengths of salt-bridge

The electrostatic strengths of salt-bridges is calculated as described in Sinha et al. 2002 [24]. The electrostatic contributions of salt-bridges to the free energy of folding and binding were calculated relative to their hydrophobic

isosteres. Hydrophobic isosteres of a salt-bridge result when the partial atomic charges on the side-chain atoms are set to zero. The method utilizes a continuum electrostatic approach, as described by Hendsch and Tidor 1994 [38], to solve linearized Poisson–Boltzmann equation, using DELPHI computer program developed by Honig and co-workers [39, 40]. The method has been widely used [38, 41, 42] and experimentally verified [43, 44]. DELPHI available at the Insight II interface was utilized for the calculations. The electrostatic contributions upon salt-bridge formation can be derived from three components: (i) $\Delta\Delta G_{desol}$: The term represents sum of the desolvation penalties paid by the salt-bridging side-chains, when they are brought from the dielectric of 80.00, in water, to the dielectric of 4.0, in the protein interior; (ii) $\Delta\Delta G_{bridge}$: This term represents the favorable stabilizing energy due to opposite charges of salt-bridging side-chains; (iii) $\Delta\Delta G_{protein}$: The term delineates the electrostatic interactions of salt-bridging side-chains with the charges in the rest of the protein, to evaluate the favorability or unfavorability of protein environment for that particular salt-bridge. Accounting the above three terms allow us to simulate the free energy difference of the salt-bridge, between unfolded and folded/bound and unbound structure. The total electrostatic energy upon the salt-bridge formation would be:

$$\Delta\Delta G_{tot} = \Delta\Delta G_{desol} + \Delta\Delta G_{bridge} + \Delta\Delta G_{protein}$$

DELPHI sofware package calculates the electrostatic potential in and around macromolecule, using finite difference solution to the Poisson–Boltzmann equation. The desolvation penalty of a salt-bridging side-chain is the difference between its reaction field energy in water and in protein. Linearized Poisson–Boltzmann equation was solved, using DELPHI, to estimate the potential created due electrostatic interactions of salt-bridging side-chains. The electrostatic potential of a salt-bridging side-chain was multiplied by its charges to estimate the bridge term. Similarly linearized Poisson–Boltzmann equation was solved, using DELPHI, to estimate the electrostatic potential created on the protein by the salt-bridging side-chains. The electrostatic potential was multiplied by the charges of the protein to estimate the protein term. The total electrostatic strength of the salt-bridge was the sum of these three terms.

When estimating the protein term the charges except that of salt-bridging side-chains were set to zero. In the case of bridge term calculation one of the salt-bridging side-chain contained its charges, while the rest of the charges were set to zero. The method is described in details in Hendsch & Tidor, 1994 [38].

The protein structure was mapped on $79 \times 79 \times 79$ point three-dimensional grid for iterative finite difference calculations. Hydrogen atoms were added to the structures and the protonation state of the charged residues were defined, at pH 7.0, using the BIOPOLYMER module of INSIGHT II (release 98.0 from Molecular Simulations, Inc). PARSE3 set of atomic charges and radii [45] were used. Solvent probe radius of 1.4 Å was used. The dielectric constant of solute (protein) was kept 4.0 and that of solvent was kept 80.00. The ionic strength of 145 mM was used, to simulate the physiological conditions as much as possible. The output energy value in units kT, where k is the Boltzman constant and T is the absolute temperature, were multiplied with the conversion factor 0.592 to obtain the results in kilo calories per mole at room temperature, 25°C. For each calculation, the structures were first mapped on the grid where molecule occupied 50% of the grid and Debye–Huckel boundary conditions were applied [46]. The resulting rough calculations were used as a boundary condition for focused calculation, where molecule extent was kept 95% on the grid. The results of focussed calculations are shown here.

Alanine scanning of charged epitope residues

Alanine mutations were made on HEL charged residues in or near the H63 epitope, and the mutant lysozymes expressed in *Pichia pastoris* and purified as described previously. Fab63 was expressed in E. coli and purified as described [16]. HEL or mutant HEL was amine-coupled to research grade CM-5 sensor chips (BIAcore, Inc., Piscataway, NJ), and binding kinetics of Fab63 recorded at 25°C in a BIAcore1000 or BIAcore2000 biosensor as previously detailed [23, 47]. Equilibrium constants for each complex were calculated from rate constants obtained using a two-step model [23, 47]. The free energy change of association of each complex was calculated from the respective equilibrium constant using the relationship G = –RTln(Ka). The change in free energy attributable to each mutation was calculated as:

$$\Delta\Delta G_{mut-HEL} = \Delta G_{mut} - \Delta G_{HEL}$$

Results and discussion

Binding ‘‘hot-spots’’ in HH-HEL complexes

X-ray crystal structures are available for HH10-HEL, HH63-HEL, and HH26-HEL complexes, but not for HH8-HEL. HH26-HEL, as well as HH8-HEL have been homology modeled using HH10-HEL as template [48]. The Fv of the HH26-HEL crystal structure and the model are similar, with an RMSD (1.03 Å) within the resolution of the X-ray structure of, and have similar molecular interactions (Table 1) [48]. Thirteen non-glycine HEL residues

Table 1 Salt-bridges in HH8-HEL, HH10-HEL, HH26-HEL and HH63-HEL complexes, in free HH63 and free HEL, and in the conformers extracted from in vacuo and explicit MD simulations

Salt-bridge	HH-HEL Complex					Uncomplexed		200 ps in vacou	20 ps explicit
	HH8	HH10	HH26		HH63	HH63	HEL	MD simulation HH63-HEL conformer	MD simulation HH63-HEL conformer
			M	X					
Inter-molecular									
$Asp32_H$-$Lys97_Y$	✓	–	✓	✓	–	–	–	✓	✓
$Glu99_H$-$Lys97_Y$			✓		–	–	–	–	–
Intra-molecular: Antibody									
$Lys49_L$-$Asp101_H$	–	–	–		–	✓	–	✓	✓
$Asp99_H$-$His34_L$	–	✓	–		–	–	–	–	–
$Asp99_H$-$Lys49_L$	–	✓	–		–	–	–	–	–
$Lys64_H$-$Glu88_H$	✓	–	–		–	–	–	–	–
$Arg66_H$-$Asp89_H$	✓	✓	✓		✓	✓	–	–	✓
$Arg38_H$-$Glu46_H$	–	✓	–		–	–	–	–	–
$Arg97_H$-$Glu99_H$	–	–	✓		–	–	–	–	–
$Arg97_H$-$Asp101_H$	–	–	✓	✓	–	–	–	–	–
$Asp72_H$-$Lys75_H$	–	–	–		–	–	–	–	✓
$Arg24_L$-$Asp70_L$	✓	✓	✓		–	✓	–	–	✓
$Arg61_L$-$Glu79_L$	✓	✓	–	✓	–	✓	–	–	–
$Arg61_L$-$Asp82_L$	✓	✓	✓	✓	✓	✓	–	–	✓
$Lys39_L$-$Glu42_L$	–	✓	–		–	–	–	–	-
$Lys39_L$-$Glu81_L$	–	✓	–		–	–	–	–	✓
$Lys103_L$-$Glu105_L$	–	✓	–		–	–	–	–	✓
$Glu42_L$-$Arg45_L$	–	–	✓		–	–	–	–	–
$Arg45_L$-$Glu81_L$	–	–	–		–	–	–	–	✓
Intra-molecular: HEL									
$Lys1_Y$-$Glu7_Y$	–	✓	–		✓	–	✓	–	✓
$Arg14_Y$-$Asp18_Y$	–	–	–		–	–	–	✓	–
$Lys13_Y$-$Asp18_Y$	–	–	–		–	–	–	✓	–
$Asp48_Y$-$Arg61_Y$	–	–	✓		–	–	✓	✓	–
$Asp66_Y$-$Arg68_Y$	–	–	✓		–	–	–	–	–
$Asp119_Y$-$Arg125_Y$	–	✓	✓		–	–	–	–	–

Ten conformations in from each simulation were analyzed. A tick in the MD columns show the presence of that salt-bridge in one or more conformations extracted from respective MD trajectories. Salt-bridging residues are shown by their three letter residue code, followed by the residue position. One letter subscript is the chain ID (H: Heavy chain; L: Light chain; Y: Lysozyme)

Dash shows that particular salt-bridge or hydrogen-bond is absent

M: Model; X: Crystal structure

contact HH10 antibody through a salt-bridge, hydrogen-bonds and Van der Waals interactions [20]. These residues are $His15_Y$, $Tyr20_Y$, $Arg21_Y$, $Trp63_Y$, $Arg73_Y$, $Leu75_Y$, $Thr89_Y$, $Asn93_Y$, $Lys96_Y$, $Lys97_Y$, $Ile98_Y$, $Ser100_Y$ and $Asp101_Y$. In a detailed structural comparison of HH10-HEL and HH63-HEL complexes Li et al. 2000 [16] reported that the same residues contacted HH63. In addition $Arg14_Y$, $Gly16_Y$, $Asn19_Y$ and $Gly102_Y$ contacted both antibodies, and two additional residues, $Trp62_Y$ and $Asn103_Y$ contacted HH63 but were buried in HH10-HEL complex. HH8 and HH26 have the similar ''footprint'' of contacts and buried surface area on HEL as HH10 and HH63, but the structural and thermodynamic details of atomic interaction between antibody and antigen differ [21, 23, 24, 31, 32, 48].

In order to compare the details of binding specificities and to interpret functional differences among the antibodies with respect to their detailed structural differences, we performed Ala scans on all four antibodies using 16 Ala substituted HEL expressed in *Pichia pastoris* [16]. The free

energy of binding was estimated for each mutant complex from the rate constants and binding affinity as measured by SPR [23, 48]. Ala scanning results are consistent with our hypothesis that the four antibodies bind ''coincident epitopes'', with nearly identical ''footprints'' on the antigen (Fig. 1a), but the energetic contribution of each epitope residue varies among the complexes, where HH8 and HH10 are less, and HH26 and HH63 are more, sensitive towards epitope mutations. In other words the fine details of binding thermodynamics are different in these complexes

The quantitative amounts and relative ranking of individual Ala mutants of charged epitope residues were also unique for each complex (Fig. 1b). For example, mutation of $Asp18_Y$ to $Ala18_Y$ increased the binding energy strongly in HH63-HEL, but only weakly (1 kcal/mol) in the other three complexes. $Asp48_Y$ to $Ala48_Y$ also significantly increased the binding energy in HH10-HEL complex (about –1.0 kcal/mol). The residue $Lys97_Y$ is a ''hot spot'' residue in all four complexes, contributing ≥–2.0 kcal/mol) in all the complexes [24, 31]. Among the charged residues $Arg21_Y$ also contributes –2.0 kcal/mol in HH10-HEL, HH26-HEL and HH63-HEL $Arg21_Y$ forms several hydrogen-bonds in HH26-HEL, one of which is common to all four complexes [24].

Comparison of salt-bridge interactions at the binding interfaces of HH8-HEL, HH10-HEL, HH26-HEL, and HH63-HEL complexes

Salt-bridge interactions in HH-HEL complexes, and common salt-bridges in MD conformers are shown in Table 1. Asp 32_H-$Lys97_Y$, $Arg24_L$-$Asp70_L$, $Lys1_Y$-$Gly7_Y$ are the few common salt-bridges. The $Asp32_H$-$Lys97_Y$ molecular interaction is one of the ''hot-spots'' of binding in all four complexes (Fig. 1b). $Asp32_H$-$Lys97_Y$ forms an inter-molecular salt-bridge between CDR-2 of the heavy chain and the epitope residue in HH8-HEL and HH26-HEL complexes (Table 1). $Lys97_Y$ is a ''hot-spot'' residue in all 4 complexes [24] (Fig. 1, Sinha et al. 2002). Continuum electrostatic calculations show that this inter-molecular salt-bridge is stabilizing both in HH8-HEL and HH26-HEL, and in case of HH26-HEL it is exceptionally strong. In the HH26-HEL complex, $Lys97_Y$ also forms a salt-link with $Glu99_H$, and these salt-bridges are part of a salt-bridge pentad which makes a very large electrostatic contribution to the free energy of folding and binding [48]. Li et al. [16, 31, 32] and Padlan et al. [20] classified the $Asp32_H$-$Lys97_Y$ ion pairs as salt-bridges in the crystal structures HH63-HEL and HH10-HEL complexes, respectively. We used a robust method for salt-bridge assignment, including only interactions with good geometry in our salt-bridge category (detailed in Methods). Salt-bridges with good geometry are shown to have structural/functional significance [49]. The close electrostatic interactions which did not exhibit good geometry are addressed here as ion-pairs, rather than salt-bridges. The $Asp32_H$-$Lys97_Y$ interaction was classified as ion pairs rather than salt-bridges in the HH10 and HH63 complexes using our robust criterion. Although the distance between $Asp32_H$ Oδ2 and $Lys97_Y$ Nζ atoms is 2.67 Å in the case of HH63-HEL, the centroids of the charged groups are not within 4 Å. The $Asp32_H$-$Lys97_Y$ ion-pair is very weak in HH10-HEL complex (0.068 kcal/mol) [24]. Ala scanning analysis identify $Lys97_Y$ as a ''hot spot'' for both complexes (Fig. 1). A crystal structure of HH10Fv-HEL complex reports the presence of $Asp32_H$-$Lys97_Y$ inter-molecular salt-bridge [50]. However, since HH10Fab and HH10Fv are very different in their affinity towards HEL, HH10Fv interactions may not be representative of all HH10Fab-HEL inter-molecular interactions. During the 1Nsec explicit, 20 ps explicit and 200 ps in vacuo MD simulations the side-chains of $Asp32_H$ and $Lys97_Y$ came closer, to be qualified as a salt-bridge of a good geometry (an interaction meeting both the salt-bridging criterion, as described in Materials and Methods); their side-chains remained close with high electrostatic strength, and this good geometry salt-bridge had a high population time (described in a later section).

Salt-bridges present in unbound HH63 and HH63-HEL complex

Over-all, out of seven salt-bridges present in free HH63 and HEL, only three are retained in the complex (Table 1). This suggests inherent structural complementarity to the antigen and absence of significant local rearrangements in the region of the salt-bridges that are retained, including $Arg66_H$-$Asp89_H$, present at the binding site of free antibody. CDR-H3 undergoes conformational rearrangement, moving about 1.9 Å in the bound compared to free Fab [16] (Li et al. 2000), and an inter-chain salt-bridge, $Lys49_L$-$Asp101_H$ is lost upon HEL binding. Salt-bridge, $Arg24_L$-$Asp70_L$, present at the binding site also break upon HEL binding. This is in contrast to what is seen in HH8-HEL, HH10-HEL and HH26-HEL complexes, where the salt-bridge, $Arg24_L$-$Asp70_L$, is retained (Table 1), suggesting a structural/functional role of this salt-bridge. An intra-molecular salt-bridge $Lys1_Y$-$Glu7_Y$, not present in free HH63, is present in both HH63-HEL and HH10-HEL complexes (Table 1), indicating possible common binding mechanisms. Only the salt-bridges present in the variable domain and the HEL are shown in cases of HH8-HEL, HH10-HEL, and HH26-HEL (Table 1). Each salt-bridge present in HH63-HEL is present in at least in one of the HH8-HEL, HH10-HEL, and HH26-HEL complexes, with exception of $Lys49_L$-$Asp101_H$. In contrast, there are

intra-molecular salt-bridges in the other three complexes which are not found in HH63-HEL (Table 1). The important inter-molecular salt-bridges [24] present in structures of HH8-HEL, HH10-HEL, and HH26-HEL complexes are not present in HH63-HEL complex structure (Table 1).

Salt-bridges predicted to be of structural/functional importance are revealed during the MD simulations of HH63-HEL

In order to examine the dynamics of molecular interactions and their structural significance, conformations extracted from previously published 1 Nsec MD trajectory of HH63-HEL complex [34] were studied. In addition, we have also studied 200 ps in vacuo MD simulation. Conformations extracted from an independent 20 ps explicit MD simulation were also analyzed. Conformations from independent simulations were analyzed mainly to further check the validity of the revealed interactions. Further, the electrostatic strength of these salt-bridges were computed as described by Hendsch and Tidor, by solving Poisson–Boltzmann equation using sofware DELPHI, developed by Honig and coworkers [39, 40].

Eleven salt-bridges, not present in the X-ray crystal structure, are revealed during 1 Nsec simulation. $Glu46_H$-$His60_H$ and $Lys1_Y$-$Asp87_Y$ are formed only once, and are not present in any other HH-HEL complexes, and are not revealed during any other short simulations. It is likely that these salt-bridges were formed due to local fluctuations of sade-chains, and so may not be of structural and functional significance. All the salt-bridges, except two, are present in at least one of the HH complexes (Table 1 and 2). Many of the intra- and inter-molecular salt-bridges, not present in the X-ray structure, are acquired during MD run. Two inter-molecular salt-bridges are revealed. There are two newly formed salt-bridges, which are not present in either HH complexes or HH63 crystal structures. One inter-molecular salt-bridge, $Asp101_H$-$Lys97_Y$, and one intra-molecular salt-bridge, $Arg45_L$-$Asp82_L$, are newly acquired.

The in vacuo and 20 ps explicit simulations revealed similar patterns of salt-bridges (Tables 1, 3). During the MD simulations, both in vacuo and 20 ps explicit (Table 1, 3), important salt-bridges were revealed. $Asp32_H$-$Lys97_Y$ and $Lys49_L$-$Asp101_H$ are also revealed during in vacuo and 20 ps simulations. Three out of five salt-bridges present in the conformers of in vacuo simulation are common to salt-bridges present in at least one of the other three HH-HEL complexes. Eight out of eleven salt-bridges formed during the 20 ps MD simulation, are present in at least one of the other three complexes. Most of the intra-molecular salt-bridges formed in the MD conformers are present in the crystal structures of uncomplexed HH63 or HEL. The acquired salt-bridges recur in conformers of the MD simulation. For example, $Asp32_H$-$Lys97_Y$ is present in three out of ten observed conformers in case of in vacuo simulation, and in nine out of ten observed conformers in case of explicit simulation. Importantly, inter-molecular salt-bridge, $Asp32_H$-$Lys97_Y$, and interchain salt-bridge, $Lys49_L$-$Asp101_H$, are revealed in all the simulations. Both the salt-bridges have high population time. Structural and functional importance of these interactions are discussed in later sections. Similarly in cases of explicit simulations most of the acquired salt-bridges are present in significant numbers of observed conformations (Table 2 & 3).

Inter-molecular salt-bridge $Asp32_H$-$Lys97_Y$

Seventeen out of twenty examined conformations reveal the presence of the inter-molecular salt-bridge- $Asp32_H$-$Lys97_Y$, in 1 Nsec explicit simulation. Additionally this intermolecular salt-bridge forms a salt-bridge triad in three conformations (Table 2, Fig. 2). In the HH26-HEL complex, the $Asp32_H$-$Lys97_Y$ salt-bridge is part of an inter-molecular pentad, which makes a large electrostatic contribution to the binding energy [24]. In contrast HH8-HEL and HH10-HEL complexes does not contain any inter-molecular salt-bridge networks [24]. HH10-HEL complex contains an intra-molecular salt-bridge network [24]. Salt-bridge networks have been shown to play important structural and functional roles [24]. It has been proposed salt-bridge networks are electrostaically favorable towards folding and binding, and they render the site very specific for an efficient binding. This is consistent with the proposal that HH63-HEL binding is similar to HH26-HEL binding, in terms of epitope mutant specificity and its electrostatic properties.

Nine out of ten conformations from the 20 ps explicit MD simulation trajectory and 3 out of 10 conformations from in vacuo simulations also reveal the presence of $Asp32_H$-$Lys97_Y$ inter-molecular salt-bridge. This salt-bridge once formed, remains intact throughout the simulation. This salt-bridge has a high population time, as shown in all the simulations. $Asp32_H$-$Lys97_Y$ is stabilizing in all the conformers of HH63-HEL (Table 3), fluctuating from –2.145 to –4.959 kcal/mol in 200 ps simulation, and has a strength of –1.479 kcal/mol at 20 ps timestep of explicit simulation. These values correlate with Ala scanning data, which suggests a net free energy contribution of Lys97 to be nearly –4.0 kcal/mol (Fig. 1). The epitope residue $Lys97_Y$ is a ''hot spot'' residue for binding in all the four complexes (Fig. 1). This salt-bridge is weak (–2.00 kcal/mol) in HH8-HEL, where the binding is cross-reactive, and very strong (–7.78 kcal/mol) in HH26-HEL, where the binding is very specific [24]. High specificity between HH26 and HEL has been proposed due to very electrostatic nature of their binding [24].

Table 2 Revealed salt-bridges, and their recurrence, during 1NSec MD simulations

Salt-bridge	800	810	820	830	840	850	860	870	880	890	900	910	920	930	940	950	960	970	980	990	1000
Inter-molecular																					
$Asp32_H$-$Lys97_Y$	✓	✓	✓	✓	✓	✓	✓	✓	✓	✓	✓		✓		✓	✓		✓	✓		✓
$Asp101_H$-$Lys97_Y$									✓	✓	✓										
Intra-molecular: Antibody																					
$Lys49_L$-$Asp101_H$	✓		✓	✓	✓																
$Asp72_H$-$Lys75_H$		✓	✓	✓																	
$Glu46_H$-$His60_H$														✓							
$Arg24_L$-$Asp70_L$									✓	✓		✓			✓	✓					✓
$Lys103_L$-$Glu105_L$										✓	✓										
$Arg45_L$-$Asp82_L$						✓		✓													
$Lys39_L$-$Glu42_L$				✓								✓			✓	✓		✓			
Intra-molecular: HEL																					
$Lys1_Y$-$Glu7_Y$	✓	✓	✓	✓			✓	✓	✓	✓		✓					✓				
$Lys1_Y$-$Asp87_Y$																			✓		
$Lys13_Y$-$Asp18_Y$						✓						✓		✓		✓	✓	✓	✓	✓	

Salt-bridging residues are shown by their three letter residue code, followed by the residue position. One letter subscript is the chain ID (H: Heavy chain; L: Light chain; Y: Lysozyme). The presence of the particular salt-bridge in a conformations are shown by ticks

Table 3 Recurrence of salt-bridges during in vacuo and explicit MD simulations

Salt-bridge	In vacou Timesteps (ps)										20 ps Explicit Timestep (ps)									
	110	120	130	140	150	160	170	180	190	200	11	12	13	14	15	16	17	18	19	20
Inter-molecular																				
$Asp32_H$-$Lys97_Y$	✓							✓		✓		✓	✓	✓	✓	✓	✓	✓	✓	✓[a]
Intra-molecular: Antibody																				
$Lys49_L$-$Asp101_H$		✓	✓			✓			✓			✓		✓	✓			✓		
$Arg66_H$-$Asp89_H$											✓					✓				
$Asp72_H$-$Lys75_H$																		✓	✓	
$Arg24_L$-$Asp70_L$															✓					
$Arg61_L$-$Asp82_L$											✓	✓			✓	✓		✓		✓
$Lys39_L$-$Glu81_L$											✓	✓				✓	✓	✓	✓	✓
$Lys103_L$-$Glu105_L$											✓	✓		✓	✓	✓	✓	✓	✓	
$Arg45_L$-$Glu81_L$												✓			✓		✓		✓	
Intra-molecular: HEL																				
$Lys1_Y$-$Glu7_Y$											✓	✓	✓	✓	✓	✓	✓	✓	✓	✓
$Arg14_Y$-$Asp18_Y$		✓	✓	✓						✓										
$Lys13_Y$-$Asp18_Y$			✓	✓																
$Asp48_Y$-$Arg61_Y$				✓																

Salt-bridging residues are shown by their three letter residue code, followed by the residue position. One letter subscript is the chain ID (H: Heavy chain; L: Light chain; Y: Lysozyme). The presence of the particular salt-bridge in a conformations are shown by ticks

[a] Electrostatic strength is –1.479 kcal/mol

An additional inter-molecular salt-bridge, $Asp101_H$-$Lys97_Y$, is revealed in HH63-HEL during 1Nsec MD simulation. $Asp101_H$ forms an important inter-chain salt-bridgewith $Lys49_L$.It is interesting to note that $Asp101_H$ fluctuates to between forming inter-molecular salt-bridge and intra-molecular salt-bridge (Fig. 2a, b). Conformations at 800, 820, 830 and 840 ps time steps reveales its participation in inter-chain salt-bridge. Conformations at 880, 890 and 900 ps time steps it participates in the formation of inter-molecular triad (Fig. 2). Interestingly the inter-chain salt-bridge is also present in uncomplexed HH63 (Table 1). An electrostatic interaction between $Lys49_L$ and $Asp101_H$

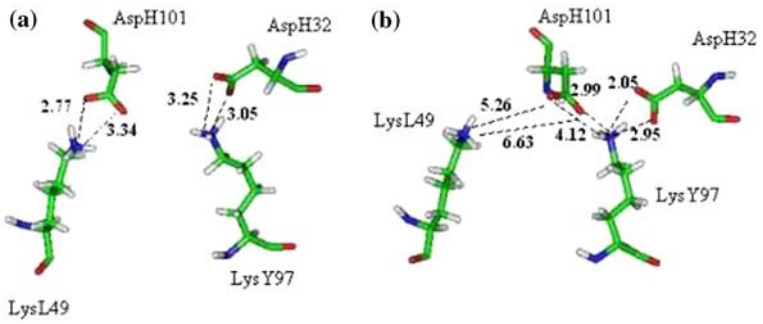

Fig. 2 Fluctuation between inter and intra-molecular triad in HHH63-HEL, as revealed during 1 Nsec MD simulation. $Asp101_H$, which forms an inter-chain salt-bridge with $Lys49_L$ at 800 Nsec time step (**a**), breaks to form inter-molecular salt bridge triad with $Lys97_Y$, shown in conformation at 880 Nsec time step (**b**). Distances are shown in Å

has been reported in case of HH10-HEL complex [48]. Light chain and heavy chain undergo conformational changes, relative to each other, upon HEL binding [51]. Breaking of $Lys49_L$-$Asp101_H$ salt-bridge to form $Asp32_H$-$Lys97_Y$-$Asp101_H$ inter-molecular salt-bridge triad further corroborates the proposal.

In contrast to $Lys97_Y$, lysine at the position 96 of HEL does not participate in salt-bridges in any of the MD conformers. In all the conformers of MD simulation $Asp32_H$ and $Lys97_Y$ side-chains fluctuate forming an ion-pair or a salt-bridge, while in none of the conformers $Asp32_H$ and $Lys96_Y$ have any such interaction (Fig. 3a, b). The side-chain of $Lys96_Y$ faces in a direction opposite to the antibody-HEL interface. This suggests that the salt-bridges formed during MD simulations are optimized and evolved molecular interactions and are not just due to local side-chain fluctuations. In addition, $Lys97_Y$ participates in an H-bond network. $Lys96_Y$ participates in a complex hydrogen bond network with L-chain residues. $Lys96_Y$ has been reported to make a significant energetic contribution to the HH63-HEL complex [16, 31]. It was hypothesized that the interactions of Lys96y with the antibody might be more dynamic than that of $Lys97_Y$. Our time-resolved simulation of the HH63-HEL complex show that the side-chains of $Lys96_Y$ and $Lys97_Y$ are both equally dynamic (Fig. 3). Calculations show that in HH8-HEL, HH10-HEL, and HH26-HEL complexes $Lys96_Y$ contributes significantly less electrostatic energy than $Lys97_Y$ [24], although binding data suggests a larger contribution for this residue in HH63-HEL [16, 31]. The thermodynamic role of $Lys96_Y$ in binding remains unresolved.

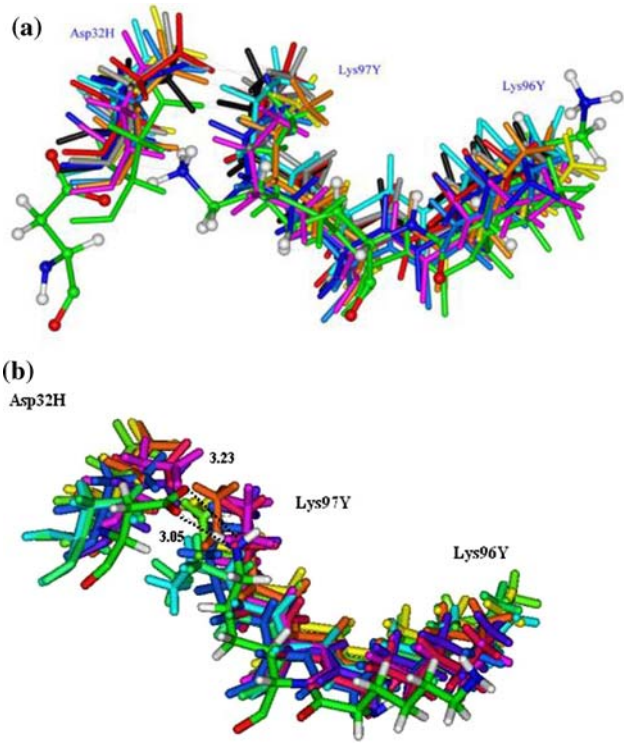

Fig. 3 Overlay of conformers to illustrate the fluctuations of side-chains of $Asp32_H$, $Lys97_Y$, and $Lys96_Y$ in 200 ps in vacuo (**a**) and 1 NSec explicit (**b**) simulation. These side-chains in the crystal structure are shown in Ball and Stick model, and are colored by atom types. The side-chains of the 10 conformers collected during the MD simulation are shown in each case. Side-chains in different color are snap shots at 110, 120, 130, 140, 150, 160, 170, 180, 190 and 200 ps of the in vacuo MD simulation. Side-chains in different color are snap shots at 800 ps, 820 ps, 840 ps, 860 ps, 880 ps, 900 ps, 920 ps, 940 ps, 960 ps, 980 and 1 NSec of the MD trajectory. The distances between $1O^{\delta}$ atom of $Asp32_H$ and N^{ζ} atom of $Lys97_Y$ are shown for conformation at 820 ps time step of 1 Nsec simulation (b)

Intra-molecular salt-bridges in HH63

1 NSec explicit simulation show the presence of eight intra-molecular salt-bridges. All of them are present in at least one of HH antibodies. $Asp72_H$-$Lys75_H$, $Arg24_L$-$Asp70_L$, $Lys103_L$-$Gly105_L$, $Lys13_Y$-$Asp18_Y$, $Lys49_L$-$Asp101_H$, and $Lys39_L$-$Glu42_L$ salt-bridges, absent in HH63-HEL X-ray structure, were revealed during simulation. These salt-bridges are present at least in one of the HH-HEL complex. Among these salt-bridges$Arg24_L$-$Asp70_D$, $Lys13_Y$-$Asp18_Y$, and $Lys49_L$-$Asp101_H$ are considered to be structurally/functionally important salt-bridges (described in later sections). Two salt-bridges, $Glu46_H$-$His60_H$, and $Arg45_L$-$Glu81_L$, only formed during 1 Nsec simulation. $Glu46_H$-$His60_H$ is only formed in one conformation, and $Arg45_L$-$Glu81_L$ is formed in two

conformations. None of these salt-bridges are present in any HH antibodies (Table 1). The insignificant population time of these-bridges suggest that these salt-bridges may have been form due to local fluctuations, and therefore, may not be playing significant structural and functional role.

During 1 Nsec simulation an inter-molecular salt-bridge, $Asp101_H$-$Lys97_Y$, is revealed with realtively high population time. In conformations at 870, 880, and 900 ps time steps HH63-HEL forms an inter-molecular salt-bridge triad involving residues $Asp32_H$, $Asp101_H$ an $Lys97_y$. This triad involves $Lys97_Y$, shown to have largest contribution, among all the epitope residues, towards HH63-HEL binding. HH26-HEL also has an inter-molecular salt-bridge triad at its binding site [24]. This triad is electrostatically very strong, and proposed to play a major role in HH26-HEL binding specificity [24]. The presence of an inter-molecular triad in HH63-HEL implies that electrostatic networking in HH63-HEL is more robust than HH8-HEL and HH10-HEL. The finding is consistent with Ala scan results which shows that HH63 is more specific towards epitope mutants than HH8 and HH10. Furthermore, results have shown that the binding is HH8 is hydrophobically driven, while in HH26 it is electrostatically. The binding mechanism in HH10 falls somewhere between HH8 and HH26. The presence of a triad is consistent with high binding specificity of HH63-HEL, and suggest its electrostically driven binding.

All eight out of nine intra-molecular salt-bridges identified in the conformers from the 20 ps MD trajectory are common to the salt-bridges present in HH8-HEL, HH10-HEL and HH26-HEL complexes (Table 1 and 3). A salt-bridge, $Arg66_H$-$Asp89_H$, is present in all four complexes and in the free HH63 antibody (Table 1), and is revealed during 20 ps MD simulation (Table 3). $Lys39_L$-$Glu81_L$ is present in HH10 and revealed during 20 ps explicit simulation. Salt-bridges, $Lys103_L$-$Glu105_L$ and $Arg24_L$-$Asp70_L$, acquired during the explicit MD simulations, are not present in the X-ray crystal structure of HH63-HEL complex. $Lys39_L$-$Glu81_L$ and $Lys103_L$-$Glu105_L$ are present in HH10-HEL complex. $Arg24_L$-$Asp70_L$ is present in all the HH complexes and in uncomplexed HH63, therefore, seem to be playing an important role. However, this salt-bridge remains undetected in the crystal structure of HH63-HEL complex. Explicit simulations reveal the presence of this salt-bridge.

$Lys49_L$-$Asp101_H$ is a significantly populated inter-chain salt-bridge revealed during the MD simulations, and is present in the conformers extracted from all simulations. It remain undetected in HH63-HEL crystal structure. It is also present in the free HH63 antibody crystal structure (Table 1, 2, 3). $Lys49_L$-$Asp101_H$ has been proposed to limit CDR flexibility and thereby decrease cross-reactivity of HH10 and HH26 antibodies [22, 24, 48]. The observation that the salt-bridge is found in unbound HH63 and is destabilizing in the HH63-HEL complex, with its value fluctuating from +1.593 kcal/mol to +3.656 kcal/mol (Table 4), suggest unfavorable inter-chain constraints and supports the observation by Li et al. [16] showing minor retraction between light and heavy chains upon complex formation. This is consistent with the hypothesis that specificity properties of these antibodies are modulated by intra-molecular salt-bridges/salt-bridge networks which limit CDR flexibility [24, 48].

Intra-molecular salt-bridges in HEL

The presence of $Lys13_Y$-Asp18 was revealed during 1Nsec simulation, with high population Time (Table 2). Salt-bridges $Arg14_Y$-$Asp18_Y$ and $Lys13_Y$- $Asp18_Y$, acquired in in vacuo simulation, are networked and involve epitope residues (Table 3). This network was not identified in crystal structures of HH10-HEL and HH63-HEL complexes. Both the salt-bridges are very stabilizing in all the HH63-HEL conformers (Table 4), where they occur, consistent with the observations that networked salt-bridges are usually stabilizing [52, 53]. At 200 ps time step $Arg14_Y$-$Asp18_Y$ attains the stability of –11.457 kcal/mol. This salt-bridge network is oriented towards HH63 light chain CDRs, and it may be that the optimizations in HH63-HEL associations organize the binding site geometry of HEL for higher specificity. However, while the network may be locally stabilizing to HEL structure, Ala mapping suggests that the net contribution of $Asp18_Y$ to HH63-HEL complex is strongly unfavorable (Fig. 1b). This may also suggest that strong $Arg14_Y$-$Asp18_Y$ interaction actually is unfavorable for the binding. This interaction is revealed only in vacou simulation. The strong electrostatic interaction may also be helped by shrinking effect due to in vacou simulation. This interaction fall apart upon the formation of an appropriate geometry for high affinity binding. This is also consistent with the fact that in none of the conformations extracted from 1 Nsec MD simulations this salt-bridge is present

The importance of this strong network may relate to the HH63-HEL binding specificity. Double mutant cycle analysis with these three HEL residues as well as the respective contact residues on HH63 would be required to determine whether the observed destabilizing effect of Asp18 on complex formation is direct, through an unfavorable interaction with the antibody, or indirect through local folding effects on HEL.

Intra-molecular salt-bridge $Asp48_Y$-$Arg61_Y$ present in the conformer at 140 ps time step is also present in free HEL, though absent in the HH63-HEL X-ray crystal

Table 4 Electrostatic strengths of salt-bridges in the conformers extracted from in vacuo MD simulation

Salt-bridge	110	120	130	140	150	160	170	180	190	200
Inter-molecular										
$Asp32_H$-$Lys97_Y$	–3.906							–2.145		–4.959
Intra-molecular										
$Lys49_L$-$Asp101_H$		2.845	2.615			1.593			3.656	
$Arg14_Y$-$Asp18_Y$		–3.073	–1.452	–4.874						–11.457
$Lys13_Y$-$Asp18_Y$			–5.458	–5.855						
$Asp48_Y$-$Arg61_Y$				2.204						

Electrostatic strengths are in units kcal/mole. Salt-bridging residues are shown by their three letter codes, followed by the residue position. Chain ID are shown in sub-script. The electrostatic contribution of a salt-bridge to the free energy of folding was computed employing the finite difference method to solve Poisson–Boltzman equation, as described by Hendsch and Tidor [38], using program DELPHI, developed by Honig and co-workers [39, 40]

structure (Table 1). This salt-bridge is also present in the HH26-HEL complex [24], but is absent in the structures of HH8-HEL, HH10-HEL and HH63-HEL (Table 1). The presence of this salt-bridge in uncomplexed HEL and HH26-HEL complex was postulated to indicate very specific binding between HH26 and HEL [24]. $Asp48_Y$ does not contact the antibody in either HH26-HEL or HH63-HEL. The Ala scanning data suggests that $Asp48_Y$ makes only a weak contribution to binding energy (less than –1.0 kcal/mol) in both complexes. This may be due to the stabilization of local folding, or it could reflect a long range direct effect.

$Lys1_Y$-$Glu7_Y$ is present in free HEL, and in HH10-HEL and HH63-HEL complexes. $Lys1_Y$-$Glu7_Y$ has a high population time in the explicit simulations. Its presence in free HEL as well as in complex suggest that this salt-bridge has an important structural role. It may be contributing towards a specific geometry for the binding.

Conclusions

MD approaches have been utilized to understand molecular interactions [54–57]. MD Study has suggested impacts of a salt-bridge formation in functionally relevent conformational changes [58]. Here we show for the first time that MD simulations provide a dynamic description of molecular interactions in solution that complement and expand information inferred from the X-ray structure. 1 Nsec with periodic boundary conditions, 200 ps *in vacuo*, and and an independent 20 ps explicit MD simulations have shown the presence of significant inter and intra-molecular salt-bridges, not detected in available X-ray crystal structures. Many of the revealed salt-bridges are present in at least one of three HH-HEL complexes that belong to the same family, recur in large number of ''snap-shots'' (conformers) of the MD trajectory, and make significant thermodynamic contributions in the HH63-HEL conformers. They involve charged residues which Ala scanning experiments have identified to be ''hot spot'' residues, involved in important inter and intra-molecular contacts (Table 1 & 2, Fig. 1) (Smith-Gill et al. unpublished results) [16, 21, 22, 24, 50, 59, 60]. The results/observations suggest these interactions play a significant role in antibody- HEL binding, either directly, or indirectly through modulation of local folding of one of the components. These ''hot spot'' interactions, with high population times during MD simulation represents ''hot-spot'' molecular interaction in the solution.

The importance of salt-bridges in protein function, stability, and movements has been widely realized [13, 24, 27, 30, 41, 42]. Salt-bridges can be stabilizing [49, 41, 14], destabilizing [38, 43], or neutral [61, 62]. Whereas a salt-bridge with neutral strength may not be of functional importance, salt-bridges of both stabilizing and destabilizing strengths play important roles. Stabilizing salt-bridges may determine specificity, and destabilizing ones may also modulate the binding geometry for better fit. Salt-bridges are pin-pointed expression of electrostatic complementarities at the binding sites. The electrostatic strengths of salt-bridges has been reported to be as high as –13.00 kcal/mol. H-Bonds, although much higher in number for a given protein, usually have strengths between –2 and –4 kcal/mol. Therefore, salt-bridges can be a major determining factor for binding complementarity and specificity. In order to understand molecular recognition or affinity maturation it is extremely important that all important salt-bridges are investigated. Under dynamic conditions, the restrains put on side-chains due to crystal conditions are released, allowing side-chain interactions, which may result in the formation of a potential salt-bridge. Revelation of a salt-bridge in water, in vacuo and under the periodic boundary conditions would mean that the salt-bridge formation occurred mainly due to the release of physical constrains put during crystallization process. Dynamics, whether explicit or *in vacuo*, releases that constrain.

Stabilizing and destabilizing salt-bridges both have functional values. For example, the strongly destabilizing effect of $Asp18_Y$ revealed by Ala scanning may be derived from its participation in an intra-molecular salt-bridge network which must be broken complex association. The fact that the inter-chain salt-bridge, $Lys49_L$-$Asp101_H$, is destabilizing in all the conformers suggest that light and heavy chains may undergo slight retraction from each other during the complex formation with HEL. On the other hand, the strong electrostatic strength and high population time of inter-molecular salt-bridge $Asp32_H$-$Lys97_Y$ (Fig. 3), is consistant with experimental evidence that $Lys97_Y$ is an epitope''hot-spot'' epitope residue. The inter-molecular salt-bridge is very stabilizing in all the conformers, suggesting that the binding is electrostatically driven in this complex. Analysis of binding kinetics suggests that the electrostatics play a significant role in stabilization of the encounter complex. Our preliminary electrostatic calculations on HH63-HEL complex agree with this hypothesis [63].

Structural comparison and continuum electrostatic calculations [24] predicts some of these salt-bridges to be linked with flexible and rigid binding mechanisms in HH8-HEL, HH10-HEL, and HH26-HEL). The numbers of salt-bridges, their networking patterns, and their electrostatic strengths in these complexes correlate with and may partially determine flexibility and specificity of binding [24, 48]. The same salt bridges exhibit high population times in the MD simulation conformers of HH63-HEL.

Conformers of higher population time correspond to functionally important conformations in solution. The ''snap-shot'' conformations obtained from the X-ray crystallography may not necessarily the one with higher or highest population time, especially considering that the crystallization conditions may lead to shifts in conformational equilibrium [64]. Thus conformation of the crystal structure may not show all the details of molecular interactions. As a consequence some very important molecular interactions might be overlooked in the X-ray crystal structure. At the same time some molecular interactions, which may not be important, may show up in the structure. Thus, MD simulations may be used to identify important atomic interactions within large protein–protein complexes, even in the complexes where crystal structures are available at only moderate resolution [48].

Earlier work on the same family of antibodies has shown the importance of electrostatics on determining binding specificity and affinity [24, 63]. High specificity antibody not only forms larger number of salt-bridges with its antigen, but these salt bridges were electrostatically stronger, compared to the salt-bridges in antibody less specific towards its antigen. Through knowledge of electrostatic interactions and their thermodynamic strengths is a prerequisite in understanding the determinants of binding affinity/specificity. Previously, based on observations from 1 Nsec simulation, we show that HyHEL63 binding side is a mosaic of flexible and rigid regions. Here we analyze 1 Nsec trajectory to pin-point the formation and recurrence of salt-bridges. All different types of simulations show that the salt-bridges of high population time are structurally/functionally relevant. Most of the important salt-bridges were not revealed in the X-ray structure. Fine electrostatic-hydrophobic compensations determine protein folding and binding. Such compensations can be understood only after we have taken protein flexibilities into account. Protein functional movements, governed by flexibilities [14, 64], may shift the populations of molecular interactions. A molecular interaction can be considered functionally important only when it poses high population time in dynamic environment.

Acknowledgments We thank Prof. Ruth Nussinov for her valuable comments. We thank Prof R. A. Mariuzza for providing HyHel63-HEL structure co-ordinates, before its release in the PDB. We thank the Advanced Biomedical Computing Center personnel are thanked for computational resources, and related assistance. We thank the personnel at FCRDC are thanked for their assistance.

References

1. Kabat, E. A., Wu, T. T., & Bilofsky, H. (1977). Unusual distributions of amino acids in complementarity-determining (hypervariable) segments of heavy and light chains of immunoglobulins and their possible roles in specificity of antibody-combining sites. *Journal of Biological Chemistry, 252*, 6609–6616.
2. Dall'Acqua, W., Goldman, E. R., Lin, W., Teng, C., Tsuchiya, D., Li, H., Ysern, X., Braden, B. C., Li, Y., Smith-Gill, S. J., & Mariuzza, R. A. (1998). A mutational analysis of binding interactions in an antigen-antibody protein-protein complex. *Biochemistry, 37*, 7981–7991.
3. Wilson, I. A., & Stanfield, R. L. (1993). Antibody-antigen interactions. *Current Opinion in Structural Biology, 3*, 113–118.
4. Braden, B. C., & Poljak, R. J. (1995). Structural features of the reactions between antibodies and protein antigens. *FASEB Journal, 9*, 9–16.
5. Smith-Gill, S. J. (1991). Protein-protein interactions: structural motifs and molecular recognition. *Current Opinion in Biotechnology, 2*, 568–575.
6. Tsumoto, K., Ueda, Y., Maenaka, K., Watanabe, K., Ogasahara, K., Yutani, K., & Kumagai, I. (1994). Contribution to antibody-antigen interaction of structurally perturbed antigenic residues upon antibody binding. *Journal of Biological Chemistry, 269*, 28777–28782.
7. Davies, D. R., & Cohen, G. H. (1996). Interactions of protein antigens with antibodies. *Proceedings of the National Academy of Sciences of the United States of America, 93*, 7–12.
8. Chong, L. T., Duan, Y., Wang, Lu., Massova, I., & Kollman, P. A. (1999). Molecular dynamics and free energy calculations applied to affinity maturation in antibody 48G7.Proc. *Proceedings of the National Academy of Sciences of the United States of America, 96*, 14330–14335.

9. Novotny, J., Bruccoleri, R. E., & Saul, F. A. (1989). On the attribution of binding energy in antigen-antibody complexes McPC 603, D1.3, and HyHEL5. *Biochemistry, 28*, 4735–4749.
10. Freire, E. (1999). The propagation of binding interactions to remote sites in proteins: Analysis of the binding of the monoclonal antibody D1.3 to lysozyme. *Proceedings of the National Academy of Sciences of the United States of America, 96*, 10118–10122.
11. Janin, J., & Chothia, C. (1990). The structure of protein-protein recognition sites. *Journal of Biological Chemistry, 265*, 16027–16030.
12. Jones, S., & Thornton, J. M. (1996). Principles of protein-protein interactions. *Proceedings of the National Academy of Sciences of the United States of America, 93*, 13–20.
13. Sinha, N., Tsai, C. J., & Nussinov, R. (2001). A proposed structural model for amyloid fibril elongation: Domain swapping forms an interdigitating -structure polymer. *Protein Engineering, 14*, 93–103.
14. Sinha, N., Kumar, S., & Nussinov, R. (2001). Inter-domain interactions in hinge-bending transitions. *Structure: Folding & Design, 9*, 1165–1181.
15. Carugo, O., & Argos, P. (1997). Protein-protein crystal-packing contacts. *Protein Science, 6*, 2261–2263.
16. Li, Y., Li, H., Smith-Gill, S. J., & Mariuzza, R.A. (2000). Three-dimensional structures of the free and antigen-bound Fab from monoclonal antilysozyme antibody HyHEL-63. *Biochemistry, 39*, 6296–6309.
17. Smith-Gill, S. J., Lavoie, T. B., & Mainhart, C. R. (1984). Antigenic regions defined by monoclonal antibodies correspond to structural domains of avian lysozyme. *Journal of Immunology, 133*, 384–393.
18. Smith-Gill, S. J., Hamel, P. A., Lovoie, T. B., & Dorrington, K. J. (1987). Contributions of immunoglobulin heavy and light chains to antibody specificity for lysozyme and two haptens. *Journal of Immunology, 139*, 4135–4144.
19. Newman M. A., Mainhart C. R., Mallett C. P., Lavoie T. B., & Smith-Gill, S. J. (1992). Patterns of antibody specificity during the BALB/c immune response to hen eggwhite lysozyme. *Journal of Immunology, 149*, 3260–3272.
20. Padlan, E. A., Silverton, E. W., Sheriff, S., Cohen, G. H., Smith-Gill, S. J., & Davies, D. R. (1989). Structure of an antibody-antigen complex: Crystal structure of the HyHEL-10 Fab-lysozyme complex. *Proceedings of the National Academy of Sciences of the United States of America, 86*, 5938–5942.
21. Lavoie, T. B., Mohan, S., Lipschultz, C. A., Grivel, J-C., Li, Y., Mainhart, C. R., Kam-Morgan, L. N. W., Drohan, W. N., & Smith-Gill, S. J. (1999). Structural differences among monoclonal antibodies with distinct fine specificities and kinetic properties. *Molecular Immunology, 36*, 1189–1205.
22. Lavoie, T. B., Drohan, W. N., Smith-Gill, S. J. (1992). Experimental analysis by site-directed mutagenesis of somatic mutation effects on affinity and fine specificity in antibodies specific for lysozyme. *Journal of Immunoloy, 148*, 503–513.
23. Li, Y., Lipschultz, C. A., Mohan, S., & Smith-Gill, S. J. (2001). Mutations of an epitope hot-spot residue alter rate limiting steps of antigen-antibody protein-protein associations. *Biochemistry, 40*, 2011–2022.
24. Sinha, N., Srinivasan, M., Lipschultz, C. A., & Smith-Gill, S. J. (2002). Differences in electrostatic properties at antibody-antigen binding sites: Implications for specificity and cross reactivity. *Biophysical Journal, 83*, 2946–2968.
25. Perutz, M. F. (1970). Stereochemistry of cooperative effects in haemoglobin. *Nature, 228*, 726–739.
26. Barlow, D. J., & Thornton, J. M. (1983). Ion-pairs in proteins. *Journal of Molecular Biology, 168*, 867–885.
27. Musafia, B., Buchner, V., & Arad, D. (1995). Complex salt-bridges in proteins: statistical analysis of structure and function. *Journal of Molecular Biology, 254*, 761–770.
28. Makhatadze, G. I., Loladze, V. V., Ermolenko, D. N., Chen, X., & Thomas, S. T. (2003). Contribution of surface salt-bridges to protein stability: guidelines for protein engineering. *Journal of Molecular Biology, 327*, 1135–1148.
29. Yip, K. S. P., Britton, K. L., Stillman, T. J., Lebbink, J., DeVos, W. M., Robb, F. T., Vetriani, C., Maeder, D., & Rice, D. W. (1998). Insights into the molecular basis of thermal stability from the analysis of ion pair networks in the glutamate dehydrogenase family.Eur. *Journal of Biochemistry, 255*, 336–346.
30. Kumar, S., Buyong, M., Tsai, C. J., & Nussinov, R. (2000). Electrostatic strengths of salt-bridges in thermophilic and mesophilic glutamate dehydrogenase monomers. *Proteins: Structure, Function and Genetics, 38*, 368–383.
31. Li, Y. L., Urrutia, M., Smith-Gill, S. J., & Mariuzza, R. A. (2003). Dissection of binding interactions in the complex between the anti-lysozyme antibody HyHEL-63 and its antigen. *Biochemistry, 42*, 11–22.
32. Li, Y., Li, H., Yang, F., Smith-Gill, S. J., & Mariuzza, R.A. (2003). X-ray snapshots of affinity maturation in an antigen-antibody protein-protein interfact. *Nature Structural Biology, 42*, 11–22.
33. Bernstein, F. C., Koetzle, T. F., Williams, G. J., Meyer. E. E Jr, Brice, M. D., Rodgers, J. R., Kennard, O., Shimanouchi, T., Tasumi, M. (1977). The protein data bank: a computer-based archival file for macromolecular structures. *Journal of Molecular Biology, 112*, 535–42.
34. Sinha, N., & Smith-Gill, S. J. (2005). Molecular dynamics simulation of a high-affinity antibody-protein complex: The binding site is a mosaic of locally flexible and preorganized rigid regions. *Cell Biochemistry and Biophysics, 43*, 253–274.
35. Greengard, L., & Rokhlin, V. I. (1987). A fast algorithm for particle simulations. *Journal of Computational Physics, 73*, 325.
36. Schmidt, K. E., & Lee, M. A. (1991). Implementing the fast multipole method in three dimensions. *Journal of Statistical Physics, 63*, 1223.
37. Maple, J. R., Dinur, U., & Hagler, A. T. (1988). Derivation of force fields for molecular mechanics and dynamics from ab initio energy surfaces. *Proceedings of the National Academy of Sciences of the United States of America, 85*, 5350–5354.
38. Hendsch, Z. S., & Tidor, B. (1994). Do salt bridges stabilize proteins? A continuum electrostatic analysis. *Protein Science, 3*, 211–226.
39. Gilson, M. K., & Honig, B. H. (1987). Calculation of electrostatic potential in an enzyme active site. *Nature, 330*, 84–86.
40. Gilson, M. K., Rashin, A., Fine, R., & Honig, B. (1985). On the calculation of electrostatic interactions in proteins. *Journal of Molecular Biology, 183*, 503–516.
41. Lounnas, V., & Wade, R. C. (1997). Exceptionally stable salt-bridges in cytochrome P450cam have functional roles. *Biochemistry, 36*, 5402–5417.
42. Xu, D., Lin, S. L., & Nussinov, R. (1997). Protein binding *versus* protein folding: the role of hydrophilic bridges in protein associations. *Journal of Molecular Biology, 265*, 68–84.
43. Waldburger, C. D., Schildback, J. F., & Sauer, R. T. (1995). Are buried salt-bridges important for protein stability and conformational specificity. *Nature Structural Biology, 2*, 122–128.
44. Waldburger, C. D., Jonsson, T., & Sauer, R. T. (1996). Barriers to protein folding: formation of buried polar interactions is a new slow step in acquisition of structure. *Biochemistry, 93*, 2629–2634.
45. Sitkoff, D., Sharp, K.A., & Honig, B. (1994). Accurate calculation of hydration free energies using macroscopic solvent models. *Journal of Physical Chemistry, 98*, 1978–1988.

46. Klapper, I., Hagstrom, R., Fine, R., Sharp, K., & Honig, B. (1986). Focusing of electric fields in the active site of Cu-Zn superoxide dismutase: effects ionic strength and amino acid modification. *Proteins: Structure, Function and Genetics, 1*, 47–59.
47. Lipschultz, C. A., Li, Y., & Smith-Gill, S. J. (2000). Experimental design for analysis of complex kinetics using surface plasmon resonance. *Methods, 20*, 310–318.
48. Mohan, S., Sinha, N., & Smith-Gill, S. J. (2003). Modeling the binding sites of anti-hen egg white lysozyme antibodies HyHEL-8 and HyHEL-26: an insight into the molecular basis of antibody cross-reactivity and specificity. *Biophysical Journal, 85*, 3221–3236.
49. Kumar, S., & Nussinov, R. (2002). Relationship between Ion pair geometries and electrostatic strengths in proteins. *Biophysical Journal, 83*, 1595–1612.
50. Kondo, H., Shiroishi, M., Matsushima, M., Tsumoto, K., & Kumagai, I. (1999). Crystal structure of anti-Hen egg white lysozyme antibody (HyHEL-10) Fv-antigen complex. Local structural changes in the protein antigen and water-mediated interactions of Fv-antigen and light chain-heavy chain interfaces. *Journal of Biological Chemistry, 274*, 27623–27631.
51. Schwarz, F. P., Tello, D., Goldbaum, F. A., Mariuzza, R.A., & Poljak, R. J. (1995). Thermodynamics of antigen-antibody binding using specific anti-lysozyme antibodies. *European Journal of Biochemistry, 228*, 388–394.
52. Xiao, L., & Honig, B. (1999). Electrostatic contributions to the stability of hyperthermophilic proteins. *Journal of Molecular Biology, 289*, 1435–1444.
53. Sheinerman, F. B., Norel, R., & Honig, B. (2000). Electrostatic aspects of protein-protein interactions. *Current Opinion in Structural Biology, 10*, 153–159.
54. Yang, C., Jas, G. S., & Kuczerak, K. (2004). Structure, dynamics and interaction with kinase targets: computer simulations of calmodulin. *Biochimica et Biophysica Acta, 1667*, 289–300.
55. Yu, H., Daura, X., & van Gunsteren, W. F. (2004). Molecular dynamics simulations of peptides containing an unnatural amino acid: dimerization, folding, and protein binding. *Proteins: Structure, Function and Genetics, 54*, 116–127.
56. Vaiana, A. C., Neuweiler, H., Schulz, A., Wortfrum, J., Sauer, M., & Smith, J. C. (2003). Fluorescence quenching of dyes by tryptophan: interactions at atomic detail from combination of experiment and computer simulation. *Journal of the American Chemical Society, 125*, 14564–14572.
57. Shepherd, C. M., van der Spoel, D., & Vogel, H. J. (2004). Molecular dynamics simulations of peptides from the central domain of smooth muscle caldesmon. *Journal of Biomolecular Structure & Dynamics, 21*, 555–566.
58. Liu, Y., Scolari, M., Im, W., & Woo, H-J. (2006). Protein-Protein interactions in actin-myosin binding and structural effects of R405Q mutation: A molecular dynamics study. *Proteins, 64*, 156–166.
59. Rajpal, A., & Kirsch, J. F. (2000). Role of the minor energetic determinants of chicken egg white lysozyme (HEWL) to the stability of the HEWL-antibody scFv-10 complex. *Proteins: Structure, Function and Genetics, 40*, 49–57.
60. Rajpal, A., Taylor, M G., & Kirsch, J. F. (1998). Quantitative evaluation of the chicken lysozyme epitope in the HyHEL-10 Fab complex: free energies and kinetics. *Protein Science, 7*, 1868–1874.
61. Singh, U. C. (1988). Probing the salt bridge in the dihydrofolate reductase-methotrexate complex by using the coordinate-coupled free-energy perturbation method. *Proceedings of the National Academy of Sciences of the United States of America, 85*, 4280–4284.
62. Serrano, L., Horovitz, A., Avron, B., Bycroft, M., & Fersht, A.R. (1990). Estimating the contribution of engineered surface electrostatic interactions to protein stability by using double-mutant cycles. *Biochemistry, 29*, 9343–9352.
63. Sinha, N., & Smith-Gill, S. J. (2002). Electrostatics in protein binding and function. *Current Protein & Peptide Science, 3*, 601–614.
64. Sinha, N., & Nussinov, R. (2001). Point mutations and sequence variability in proteins: Redistributions of preexisting populations. *PNAS, 98*, 3139–3144.